03,16

Low temperature cathodoluminescence in organic-inorganic perovskite $CH_3NH_3PbBr_3$ single crystals

© M.V. Akhatov[1], I.V. Zhevstovskikh[1,¶], M.N. Sarychev[2], O.I. Semenova[3]

[1] M.N. Mikheev Institute of Metal Physics, Ural Branch, Russian Academy of Sciences, Yekaterinburg, Russia
[2] Ural Federal University after the first President of Russia B.N. Yeltsin, Yekaterinburg, Russia
[3] A.V. Rzhanov Institute of Semiconductor Physics, Siberian Branch, Russian Academy of Sciences, Novosibirsk, Russia

¶ E-mail: zhevstovskikh@imp.uran.ru

Received April 11, 2024
Revised April 11, 2024
Accepted May 14, 2024

We present the results of the cathodoluminescence study in single crystals of methylammonium lead tribromide $CH_3NH_3PbBr_3$ in the low temperature orthorhombic phase (temperature range $7-100$ K). Near the edge of the optical absorption band, we found a peak at 2.24 eV that exhibited a blue shift with increasing temperature and broad emission centered at 2 eV energy, the position and intensity of which varied with the magnitude of the accelerating voltage and the direction of the electron beam. Based on Monte Carlo modeling, we have shown that for the values of the accelerating voltage used in the experiment, 1100 V and 1300 V, the penetration depth of the electron beam into the sample does not exceed 40 nm. This allows us to conclude that the observed features of the cathodoluminescence spectra are related to the properties of the near-surface layer of the $CH_3NH_3PbBr_3$ single crystal.

Keywords: organic-inorganic perovskite, cathodoluminescence, defects, Monte Carlo simulation.

DOI: 10.61011/PSS.2024.06.58708.87

1. Introduction

There is a great interest in the recent decade in studying various properties of hybrid perovskite structures, with the general formula of ABX_3; where A — methylammonium cations (CH_3NH_3, abbreviated MA) or formamidinium cations (CH_5N_2, abbreviated FA), B — metal cations (Pb, Sn), X — halogen anions (I, Br, Cl). The interest is attributable to the unique properties found in these compounds, such as the optimal value of the band gap, varied by halogen replacement, high absorption coefficient, large diffusion length of charge carriers, low exciton binding energy, as well as the simplicity and cheapness of their synthesis from a solution [1–7]. In addition, at present with the use of hybrid perovskites in solar cells as an active layer, energy conversion efficiency has been achieved by almost 26% [8–11], which is comparable to silicon analogues. These factors indicate the promise of using these compounds in photovoltaics and optoelectronics. The most common method for studying the luminescent properties of metal-organic perovskites is photoluminescence (PL) [12–17]; cathodoluminescence is much less commonly used, although cathodoluminescence (CL) is a powerful and well established method for the analysis of the recombination behavior of charge carriers in photovoltaic materials with submicrometer spatial resolution. The main specific feature of this method is locality, high sensitivity and the opportunity of layer-by-layer analysis of the sample [18,19]. A lot of material properties, including determination of energy levels of impurities or defects, dopant concentrations, charge carrier lifetimes, and defect with spatial resolution detection, can be studied using CL. However, to date there are only a few papers devoted to the study of CL in metal-organic perovskites [20–23]. Papers [20,21] studied the CL spectra of thin films $MAPbI_3$, $FAPbBr_3$, $CsPbI_3$ at a room temperature. The temperature dependences of the CL spectra of $MAPbI_{3-x}Br_x$ single crystals are presented in the paper [22], and the CL of $CH_3NH_3PbBr_3$ single crystals was studied in the paper [23] at various accelerating voltages in the range of $2-30$ kV at room temperature. Although room temperature luminescence analysis is most important for characterizing a material designed to operate in a given temperature range, lower temperatures are often used to increase the signal-to-noise ratio or to reveal in more detail optical structure that may be masked at higher temperatures due to temperature broadening of emission peaks.

In this work, we studied the CL spectra of high-quality single crystals of metal-organic perovskites $CH_3NH_3PbBr_3$ at low temperatures (in the range from 7 to 100 K) at different values of the accelerating voltage and different orientations of the electron beam with respect to the faces of the crystal, and discovered spectral features associated with defects in the near-surface layer of the sample.

2. Methods

Single crystals of metal-organic perovskite $CH_3NH_3PbBr_3$ were synthesized using a universal method of growing from a saturated solution of $CH_3NH_3PbBr_3$ powder with slow precision cooling in accordance with the technique previously presented in Ref. [24,25]. First, the precursor CH_3NH_3Br was synthesized by mixing 0.04 mol CH_3NH_2 (methylamine, 40% in aqueous solution) and 0.04 mol HBr (hydrobromic acid, 46% in aqueous solution) in the molar ratio $CH_3NH_2:HBr = 1:1$ at 0°C during stirring for 2 h. Then, 0.04 mol $PbBr_2$ was dissolved in HBr and mixed with CH_3NH_3Br, resulting in a solution from which a precipitate $CH_3NH_3PbBr_3$ precipitated. Large single crystals were grown by adding small crystals as seeds to a solution saturated at 65°C, followed by a gradual decrease of temperature, at a rate of 0.15°C per hour, to room temperature, then they were removed from the solution, washed with ether and dried. As a result, high-quality single crystals were obtained, transparent, reddish-orange in color, with typical dimensions $2 \times 3 \times 5\,mm^3$ (see inset in Figure 1).

The lattice parameter, unit cell volume and phase of $CH_3NH_3PbBr_3$ single crystals were determined by high-resolution X-ray diffractometer (Xta-LAB Synergy, Dualflex, HyPix, Rigaku Oxford diffraction) using MoK_α radiation with wavelength $\lambda = 0.71073$ Å. We are convinced that at room temperature the unit cell $CH_3NH_3PbBr_3$ has $Pm{-}3m$ cubic symmetry with lattice parameters $a = b = c = 5.92770(10)°$ Å, volume $V = 208.285(11)°$ Å^3 (the final R indices were $R_1 = 3.88\%$, $wR_2 = 10.22\%$). The obtained values are in good agreement with the previously presented data [26,27].

The temperature dependences of the CL spectra were obtained by installing the sample on a closed-cycle helium cryostat (Janis CCS-150) under a vacuum; the temperature varied from 7 to 100 K with 10 K increments. The measurements were performed in the wavelength range of 500–850 nm (energy interval 1.46–2.48 eV) with a increments of 1 nm at accelerating voltages of 1.1 and 1.3 kV, currents of 1 and 2 μA, electron diameter beam 3 mm^2 and different values (in the interval 0.4–1.4 mm) of the entrance slit of the MDR-23 monochromator, while the value of the output slit of the monochromator coincided with the input. The measurements were performed in two directions of the electron beam: *a*) perpendicular to the largest face of the sample, *b*) perpendicular to the side face (orientations are shown by arrows in the inset of Figure 1). Before starting measurements, the largest face of the sample was mechanically ground to remove the top layer of the sample by an amount of about 50 μm. This procedure was performed for reducing the impact of the effects of sample degradation under the influence of light and moisture, since PL measurements with an exciting laser wavelength of 405 nm were performed on the same single crystal before CL measurements in a wide temperature range. The side part of the sample (orientation of the type *b* in the inset of Figure 1) was not subjected to such grinding.

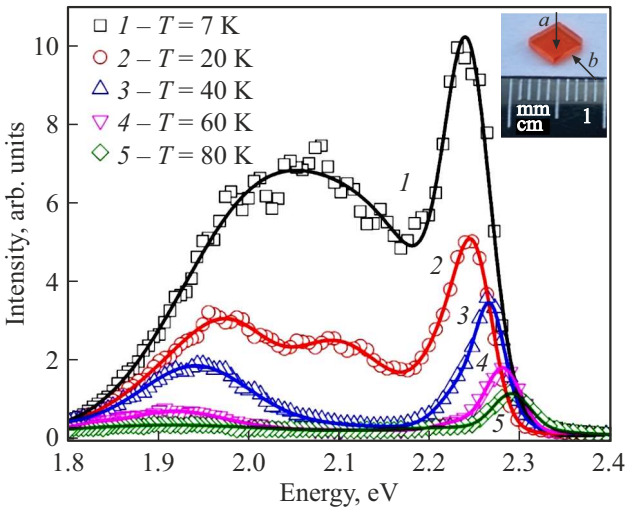

Figure 1. CL spectra in the synthesized single crystal $CH_3NH_3PbBr_3$ (shown in the inset), obtained at an accelerating voltage of 1.3 kV, current of 2 μA, entrance slit of the monochromator of 1.4 mm and the direction of the electron beam perpendicular to the largest face of the sample (corresponding to the orientation of *a* in the inset). Curve *1* — temperature $T = 7$ K, *2* — $T = 20$ K, *3* — $T = 40$ K, *4* — $T = 60$ K, *5* — $T = 80$ K.

The depth of penetration of the electron beam into the sample $CH_3NH_3PbBr_3$ was calculated based on Monte Carlo simulation [28]. The CASINO program simulates the electron trajectories by generating random numbers. It was assumed in the calculations that the deviation of the penetrating electron path during a collision is determined from the differential cross section of elastic scattering using the Rutherford formula. The initial parameters used in Monte Carlo simulations are the energy and number of electrons, the radius of the electron beam, as well as the characteristics of the substance with which the electrons interact (charge number, molar mass, material density, sample thickness).

3. Results

Figure 1 shows the CL spectra in the $CH_3NH_3PbBr_3$ single crystal, obtained with an accelerating voltage of 1.3 kV, current of 2 μA, monochromator entrance slit of 1.4 mm and at different temperatures. The electron beam was directed perpendicular to the largest face of the sample, corresponding to the type *a* orientation shown in the inset. The choice of this accelerating voltage value was determined to avoid the impact of the reabsorption effect, which manifests itself at high voltages and shifts the peak in the CL spectrum to lower energies. It was shown in Ref. [23] that the effect of reabsorption can be ignored in perovskite $CH_3NH_3PbBr_3$ at accelerating voltages below 2 kV when interpreting CL spectra.

We discovered a narrow CL peak with an energy of 2.24 eV in the studied temperature range. The position of

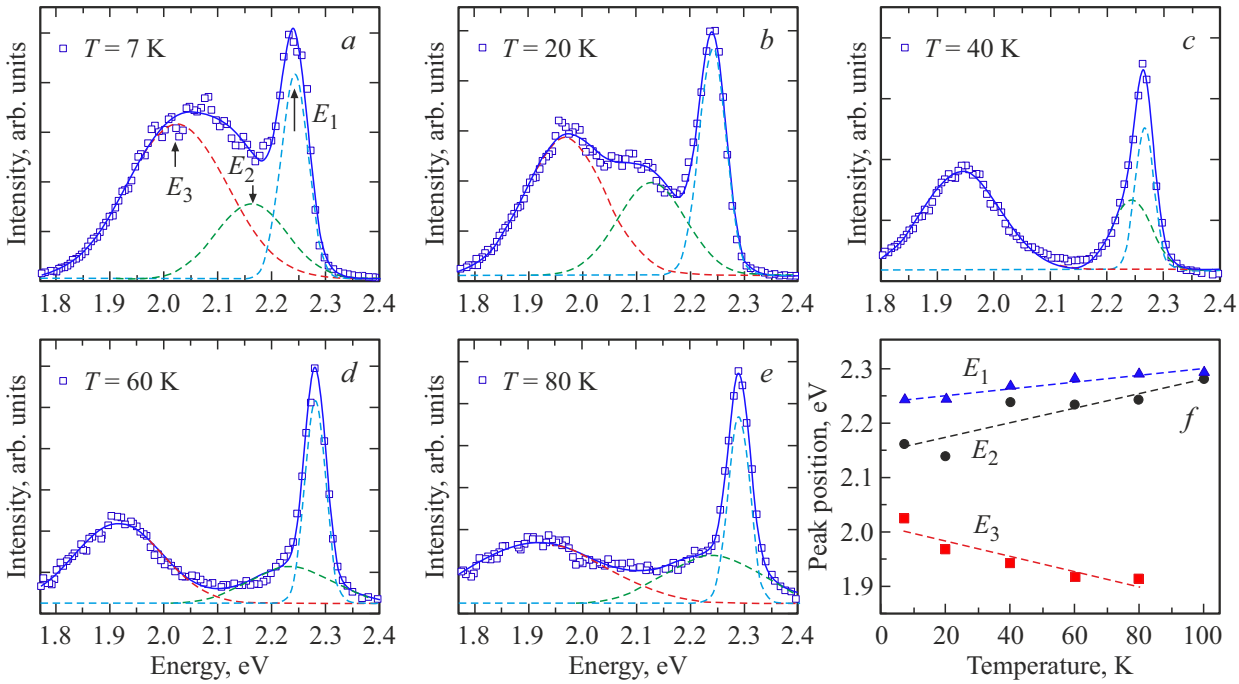

Figure 2. *a–e*) The CL spectra in the single crystal of $CH_3NH_3PbBr_3$, obtained at an accelerating voltage of 1.3 kV, current of 2 μA, monochromator entrance slit of 1.4 mm and temperatures of 7, 20, 40, 60, 80 K. Squares — experiment, lines — fitting with three Gaussian peaks E_1, E_2, E_3. *f*) Positions of maxima of E_1, E_2, E_3 peaks depending on temperature.

this peak shifted to higher energies to a value of 2.293 eV at $T = 100$ K, its intensity decreased with the increase of the temperature. The energy position of this peak is close to the band gap value, 2.258–2.292 eV in perovskite $CH_3NH_3PbBr_3$, determined by optical and magnetooptical spectroscopy methods [29–32]. In addition, we discovered a broad band in the energy range of 1.8–2.2 eV, the intensity and shape of which varied significantly with the increase of temperature, and it disappeared at a temperature of over 100 K. The temperature evolution of the CL spectra together with the fit by three Gaussian peaks is shown in Figure 2. The energies of the CL maxima are equal to $E_1 = 2.241$ eV, $E_2 = 2.161$ eV and $E_3 = 2.023$ eV at a temperature of 7 K. The positions of these peaks shifted in different ways with the increase of the temperature: E_1 and E_2 peaks shifted to higher energies (blue shift), and the peak E_3 shifted to lower energies (red shift, Figure 2,*f*).

We associate the peak with energy E_1 with the recombination of free electrons and holes near the edges of the band gap. It shifts to the blue region by an amount of approximately 50 meV with the increase of the temperature to 100 K. Similar temperature behavior was found in hybrid perovskite films $CH_3NH_3PbBr_3$ in the optical absorption spectra [32]. As for the luminescence bands with energies E_2 and E_3, their full width at half maximum is significantly larger than for the peak E_1, which may indicate a strong electron-phonon coupling and the presence of lattice defects. Previously, we observed similar wide emission bands in the PL spectra of single crystals of $CH_3NH_3PbI_3$ and $CH_3NH_3PbBr_3$ hybrid perovskites in the low-temperature orthorhombic phase [33,34]. We showed that the broad PL emission in these perovskites is attributable to the recombination of donor-acceptor pairs and coupled excitons. The defects forming the donor-acceptor pair in a crystal with iodine $CH_3NH_3PbI_3$are an interstitial cation $(CH_3NH_3)^+$ and a lead vacancy, and the interstitial iodine is a source of self-trapped excitons [33]. The most probable defects forming an donor-acceptor pair in a single crystal with bromine $CH_3NH_3PbBr_3$ are native defects — lead and bromine vacancies, forming a Schottky defect, and interstitial bromine, resulting in the formation of self-trapped excitons [34]. It should be noted that halogen vacancies are the most common point defects in metal-organic perovskites that have a low formation energy and occur during crystal growth [35].

The energies at the temperature of $T = 7$ K at which the maxima of the PL bands, $E_2 = 2.161$ eV and $E_3 = 2.023$ eV (Figure 2,*f*) are observed turned out to be close to the energies of the PL peaks $L_1 = 2.166$ eV and $L_2 = 2.132$ eV obtained at $T = 6$ K [34]. It is natural to assume that the features in the CL and PL spectra are of the same nature, since the experiments were performed on the same single crystal. We attributed the peak with energy L_1 in the PL spectra to the Schottky defect, and the peak with energy L_2 was attributed to self-trapped excitons, for which interstitial bromine is a trap [34]. However, we found different temperature behavior of the peak positions in the PL and CL spectra. Both lines with energies L_1 and L_2 demonstrated a red shift (shift to lower energies) in the PL spectra by approximately 15 and 60 meV, respectively,

with the increase of the temperature in the range of 6–60 K [34]. The band with energy E_3 also demonstrated a red shift in the CL spectra, but much stronger, by 100 meV, and the peak with the energy E_2 in the range of 7–100 K shifted to higher energies (blue shift) by a value of approximately 70 meV (Figure 2,*f*), which prevents from attributing it to emission associated with an donor-acceptor pair, which is characterized by a shift to lower energies with the increase of the temperature [34,36]. We believe that the CL band with energy E_2 can be associated, for example, with the donor– valence band transition. A shift in the position of the maximum of this band at higher energies by an amount of 70 meV with an increase of temperature from 7 to 100 K, can be attributable to ionization of the donor, and the magnitude of the shift can be considered as the approximate depth of the donor level. We determined the ionization energy of the donor– bromine vacancy using the PL spectra obtained on the same perovskite [34]; it turned out to be equal to 70 meV. Donor–valence band transition at a certain temperature will be transformed into the conduction band– valence band transition. It is clear from Figure 2,*f* that the energies of the peaks E_1 and E_2 practically coincide at $T = 100$ K. These data allow attributing the CL band with the energy E_2 to the donor – valence band transition. As for the CL band with a peak at E_3, its behavior is similar to PL emission with energy L_2 [34] and can be caused by the same defect — interstitial bromine, which is the source of self-trapped exciton states.

It should be noted that the luminescent processes occurring in CL measurements are in principle the same as in standard PL measurements: excess electrons and holes are subject to drift, diffusion and recombination through non-radiative and radiative mechanisms, regardless of whether they are excited by the electron beam (CL) or electromagnetic wave (PL). However, differences in generation between the two measurement methods may result in different information. For example, the volume of the excited substance in the case of CL can be significantly smaller than in the case of PL, and we can obtain a mismatch between the CL and PL spectra in the case of an uneven distribution of defects in the sample. The defect nature of broad emission in CL spectra is confirmed by the data shown in Figure 3.

Curves *1* and *2* in Figure 3,*a* were recorded with the orientation *a* shown in the inset of Figure 1 and different entrance slits on the monochromator. It can be seen that the CL intensity increases as the slit increases from 0.4 to 1.4 mm. The electron beam at orientation *a* fell on the sample face which was slightly polished before measurements. The curve *3* in Figure 3,*a* was obtained with the orientation *b* of the electron beam directed at the side surface of the sample, which was not polished before measurements, in contrast to the orientation *a*. It can be seen that the intensity of broad CL emission from the side face of the sample increased significantly compared to the ground face for close values of the slit (1.2 and 1.4 mm)

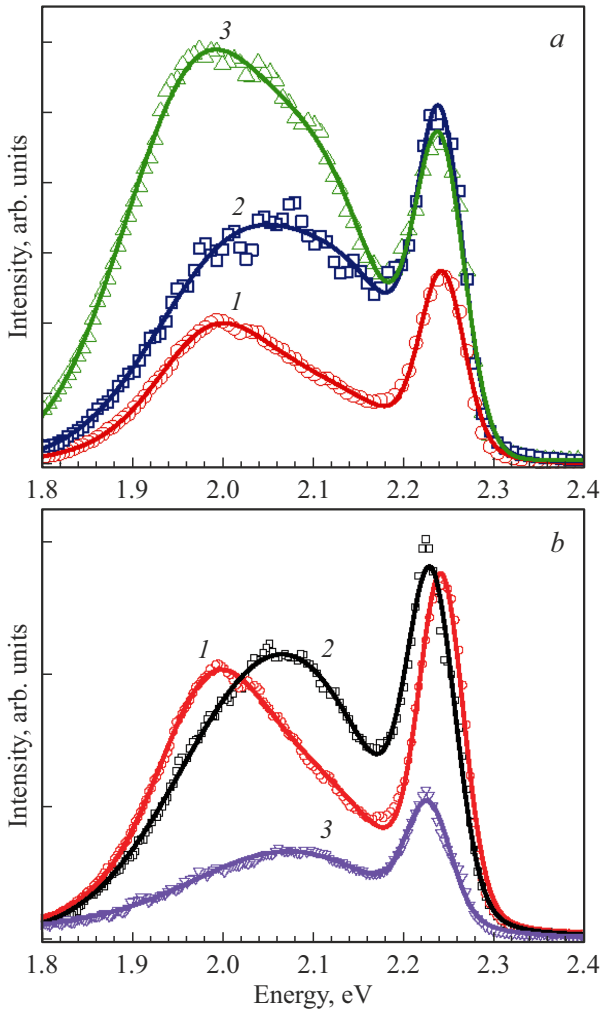

Figure 3. CL spectra in a single crystal of $CH_3NH_3PbBr_3$ obtained at a temperature of 7 K, at an accelerating voltage of 1.3 kV, current of 2 μA: *a*) curves *1* and *2* were recorded with the electron beam directed perpendicular to the largest face of the sample (orientation *a* in Figure 1) and different entrance slits on the monochromator: curve *1* — slit of 0.4 mm, curve *2* — slit of 1.4 mm; curve *3* was recorded with the beam oriented perpendicular to the side face of the sample (orientation *b* in Figure 1) and the slit of 1.2 mm; *b*) curves *1*–*3* were recorded at an orientation *a* and at various accelerating voltages: curve *1* — 1.3 kV, current of 2 μA, slit of 0.4 mm; curve *2* — 1.1 kV, current of 1 μA, slit of 0.4 mm, first measurement; curve *3* — 1.1 kV, current of 1 μA, slit of 0.4 mm, repeated measurement.

on the monochromator, which indicates a larger number of defects in the near-surface layer of the side face of the sample. Figure 3,*b* shows the CL spectra at different accelerating voltages of 1.3 and 1.1 kV (curves *1* and *2*). It should be noted that the signal intensity decreases when CL is repeatedly measured from one point of the sample, which is illustrated by the curves *2* and *3* in Figure 3,*b*. The reason for this as we believe, is that the vacuum in the measuring chamber is not high enough. The residual organic compounds under the impact of an electron beam

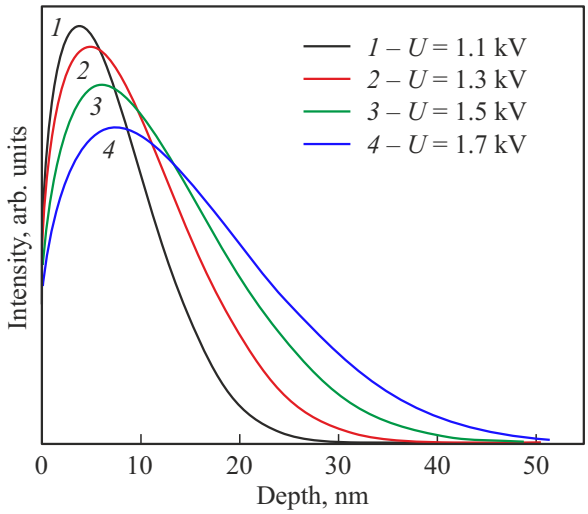

Figure 4. Results of Monte Carlo simulation in the crystal of $CH_3NH_3PbBr_3$. The CL intensity distribution is shown as a function of the distance from the sample surface; curves *1–4* correspond to different accelerating voltages.

are sorbed on the surface of the sample under the action of an electron beam, which causes complicated the penetration of the beam into the studied sample, and the CL intensity decreases. However, the ratio of peak intensities and the energy positions of the band maxima do not change.

A noticeable shift of approximately 70 meV to lower energies is observed in case of a broad emission band in the energy range 1.8–2.2 eV associated with defects. A larger near-surface region of the crystal is captured with an increase of the accelerating voltage in case of CL, and if the distribution of defects in this region is heterogeneous, this will result in changes in the CL spectra. At the same time, the characteristics of a narrow peak with energy E_1 associated with the recombination of free electrons and holes near the edges of the band gap, recorded in different orientations (*a* and *b*), at different accelerating voltages almost do not change.

Next, we performed Monte Carlo simulations to determine the depth of penetration of the electron beam into the $CH_3NH_3PbBr_3$ sample for different accelerating voltage values. We applied the following parameters for the simulation: the electron energy varied in the interval 1.1–1.7 keV with a minimum value of $E_{min} = 0.05$ keV, the number of electrons was $N_e = 10^5$, the number of paths was $N_t = 10^5$. The simulation results for the dependence of CL intensity on penetration depth are shown in Figure 4.

It can be seen that the penetration depth increases with the increase of the accelerating voltage, the maximum CL intensity is at 10 nm, the total energy of the electron beam practically does not extend to a depth of over 50 nm at these voltage values. PL spectra were obtained at an exciting laser wavelength of 405 nm in Ref. [34]; in this case, the depth of penetration of the electromagnetic field into the sample is an order of magnitude greater than in the case of CL. We believe that the observed differences in the CL and PL spectra of single crystals of $CH_3NH_3PbBr_3$ are associated with different defects forming in the near-surface layer or in the volume of the sample.

4. Conclusion

We studied the cathodoluminescence spectra of single crystals of $CH_3NH_3PbBr_3$ in the low-temperature orthorhombic phase near the optical absorption edge. We discovered a narrow peak with an energy of 2.24 eV, caused by the recombination of free electrons and holes near the edges of the band gap; its position shifted to higher energies with increasing temperature. In addition, we observed a broad emission band in the energy range of 1.8–2.1 eV at temperatures below 100 K. Based on the analysis of CL spectra recorded from different faces of the sample at various accelerating voltages, we believe that this emission is due to the presence of defects. Monte Carlo simulation showed that for the accelerating voltage values of 1100 and 1300 V used in the experiment, the depth of penetration of the electron beam into the sample is not more than 40 nm, which allows to correlate the observed features of the CL spectra with the properties of the near-surface layer of the $CH_3NH_3PbBr_3$ perovskite.

Funding

The work has been performed under the state assignment on topics „Electron“ (№122021000039-4) and „Spin“ (No. 122021000036-3). The authors from the Ural Federal University are grateful for partial support from the Ministry of Science and Higher Education of the Russian Federation (project No. FEUZ-2023-0013 and the strategic academic leadership program „Priority 2030“).

Conflict of interest

The authors declare that they have no conflict of interest.

References

[1] D.W. deQuilettes, K. Frohna, D. Emin, T. Kirchartz, V. Bulovic, D.S. Ginger, S.D. Stranks. Chem. Rev. **119**, *20*, 11007 (2019).
[2] I.E. Castelli, J.M. García-Lastra, K.S. Thygesen, K.W. Jacobsen. APL Mater. **2**, *8*, 081514 (2014).
[3] S.D. Stranks, H.J. Snaith. Nature Nanotechnol. **10**, *5*, 391 (2015).
[4] J.S. Manser, J.A. Christians, P.V. Kamat. Chem. Rev. **116**, *21*, 12956 (2016).
[5] J.H. Heo, S.H. Im, J.H. Noh, T.N. Mandal, C.S. Lim, J.A. Chang, Y.H. Lee, H.J. Kim, A. Sarkar, M.K. Nazeeruddin, M. Grätzel, S.I. Seok. Nature Photon. **7**, *6*, 486 (2013).
[6] A. Miyata, A. Mitioglu, P. Plochocka, O. Portugall, J.T.-W. Wang, S.D. Stranks, H.J. Snaith, R.J. Nicholas. Nature Phys. **11**, *7*, 582 (2015).

[7] Q. Dong, Y. Fang, Y. Shao, P. Mulligan, J. Qiu, L. Cao, J. Huang. Sci. **347**, 6225, 967 (2015).
[8] Z. Chen, B. Turedi, A.Y. Alsalloum, C. Yang, X. Zheng, I. Gereige, A. AlSaggaf, O.F. Mohammed, O.M. Bakr. ACS Energy Lett. **4**, *6*, 1258 (2019).
[9] K. Wang, D. Yang, C. Wu, M. Sanghadasa, S. Priya. Progress. Mater. Sci. **106**, 100580 (2019).
[10] K. Yoshikawa, H. Kawasaki, W. Yoshida, T. Irie, K. Konishi, K. Nakano, T. Uto, D. Adachi, M. Kanematsu, H. Uzu, K. Yamamoto. Nature Energy **2**, *5*, 17032 (2017).
[11] W. Tress. Adv. Energy Mater. **7**, *14*, 1602358 (2017).
[12] B. Wu, H.T. Nguyen, Z. Ku, G. Han, D. Giovanni, N. Mathews, H.J. Fan, T.C. Sum. Adv. Energy Mater. **6**, *14*, 1600551 (2016).
[13] Y. Liu, H. Lu, J. Niu, H. Zhang, S. Lou, C. Gao, Y. Zhan, X. Zhang, Q. Jin, L. Zheng. AIP Advances **8**, *9*, 095108 (2018).
[14] B. Wenger, P.K. Nayak, X. Wen, S.V. Kesava, N.K. Noel, H.J. Snaith. Nature Commun. **8**, *1*, 590 (2017).
[15] Y. Tian, A. Merdasa, E. Unger, M. Abdellah, K. Zheng, S. McKibbin, A. Mikkelsen, T. Pullerits, A. Yartsev, V. Sundström, I.G. Scheblykin. J. Phys. Chem. Lett. **6**, 4171 (2015).
[16] S.P. Sarmah, V.M. Burlakov, E. Yengel, B. Murali, E. Alarousu, A.M. El-Zohry, C. Yang, M.S. Alias, A.A. Zhumekenov, M.I. Saidaminov, N. Cho, N. Wehbe, S. Mitra, I. Ajia, S. Dey, A.E. Mansour, M. Abdelsamie, A. Amassian, I.S. Roqan, B.S. Ooi, A. Goriely, O.M. Bakr, O.F. Mohammed. Nano Lett. **17**, *3*, 2021 (2017).
[17] F. Staub, I. Anusca, D.C. Lupascu, U. Rau, T. Kirchartz. J. Phys. Mater. **3**, *2*, 025003 (2020).
[18] H. Guthrey, J. Moseley. Adv. Energy Mater. **10**, *26*, 1903840 (2020).
[19] L.J. Brillson. J. Phys. D **45**, *18*, 183001 (2012).
[20] C. Xiao, Z. Li, H. Guthrey, J. Moseley, Y. Yang, S. Wozny, H. Moutinho, B. To, J.J. Berry, B. Gorman, Y. Yan, K. Zhu, M. Al-Jassim. J. Phys. Chem. C **119**, *48*, 26904 (2015).
[21] C.G. Bischak, E.M. Sanehira, J.T. Precht, J.M. Luther, N.S. Ginsberg. Nano Lett. **15**, *7*, 4799 (2015).
[22] M.I. Dar, G. Jacopin, M. Hezam, N. Arora, S.M. Zakeeruddin, B. Deveaud, M.K. Nazeeruddin, M. Grätzel. ACS Photonics **3**, *6*, 947 (2016).
[23] H. Diab, C. Arnold, F. Lédée, G. Trippé-Allard, G. Delport, C. Vilar, F. Bretenaker, J. Barjon, J.-S. Lauret, E. Deleporte, D. Garrot. J. Phys. Chem. Lett. **8**, *13*, 2977 (2017).
[24] A.A. Melnikov, V.E. Anikeeva, O.I. Semenova, S.V. Chekalin. Phys. Rev. B **105**, *17*, 174304 (2022).
[25] V.E. Anikeeva, K.N. Boldyrev, O.I. Semenova, T.S. Sukhikh, M.N. Popova. Opt. Mater. X **20**, 100259 (2023).
[26] A. Jaffe, Y. Lin, C.M. Beavers, J. Voss, W.L. Mao, H.I. Karunadasa. ACS Cent. Sci. **2**, *4*, 201 (2016).
[27] C. Abia, C.A. López, L. Cañadillas-Delgado, M.T. Fernández-Diaz, J.A. Alonso. Sci. Rep. **12**, *1*, 18647 (2022).
[28] D. Drouin, A.R. Couture, D. Joly, X. Tastet, V. Aimez, R. Gauvin. Scanning **29**, *3*, 92 (2007).
[29] K. Tanaka, T. Takahashi, T. Ban, T. Kondo, K. Uchida, N. Miura. Solid State Commun. **127**, *9–10*, 619 (2003).
[30] J. Tilchin, D.N. Dirin, G.I. Maikov, A. Sashchiuk, M.V. Kovalenko, E. Lifshitz. ACS Nano **10**, *6*, 6363 (2016).
[31] K. Galkowski, A. Mitioglu, A. Miyata, P. Plochocka, O. Portugall, G.E. Eperon, J.T.-W. Wang, T. Stergiopoulos, S.D. Stranks, H.J. Snaith, R.J. Nicholas. Energy Environ. Sci. **9**, *3*, 962 (2016).
[32] F. Ruf, M.F. Aygüler, N. Giesbrecht, B. Rendenbach, A. Magin, P. Docampo, H. Kalt, M. Hetterich. APL Mater. **7**, *3*, 031113 (2019).
[33] I.V. Zhevstovskikh, N.S. Averkiev, M.N. Sarychev, O.I. Semenova, O.E. Tereshchenko. J. Phys. D **55**, *9*, 095105 (2022).
[34] I.V. Zhevstovskikh, N.S. Averkiev, M.N. Sarychev, O.I. Semenova, O.E. Tereshchenko. Phys. Rev. Mater. **8**, *3*, 034601 (2024).
[35] A. Mannodi-Kanakkithodi, J.-S. Park, A.B.F. Martinson, M.K.Y. Chan. J. Phys. Chem. C **124**, *31*, 16729 (2020).
[36] W. Stadler, D.M. Hofmann, H.C. Alt, T. Muschik, B.K. Meyer, E. Weigel, G. Müller-Vogt, M. Salk, E. Rupp, K.W. Benz. Phys. Rev. B **51**, *16*, 10619 (1995).

Translated by A.Akhtyamov